

Ionic conduction of lithium in $\text{Li}_2\text{S}-\text{SiS}_2-\text{Li}_4\text{SiO}_4$ glass system

Y. Kawakami*, H. Ikuta, T. Uchida, M. Wakihara

Department of Chemical Engineering, Tokyo Institute of Technology, Ookayama, Meguro-ku, Tokyo 152, Japan

Abstract

Chalcogenide glasses $(1-y)[0.6\text{Li}_2\text{S}-0.4\text{SiS}_2]-y\text{Li}_4\text{SiO}_4$ which are lithium ionic conductor were synthesized by a liquid nitrogen quenching method. The glass forming region of $0 \leq y \leq 0.075$ was determined by both the powder X-ray diffraction and the differential thermal analysis (DTA). From the data of DTA, the glass transition temperature (t_g) and the crystallization temperature (t_c) were maximized at $y = 0.03$ and 0.06 , respectively. Also, with the doping of Li_4SiO_4 into $\text{Li}_2\text{S}-\text{Si}_2$ glass, the stretching vibration peak for the Si–Si bridging bond slightly shifted toward higher frequency in the FT-IR spectrum. The electrical conductivity of the glass samples was measured by AC impedance method. The maximum ionic conductivity ($\sigma_{\text{RT}} = 1.5 \times 10^{-3} \text{ S cm}^{-1}$ at 25°C) was obtained at $y = 0.03$, and the activation energies (E_a) for ionic conduction increased with increasing amounts of doped Li_4SiO_4 .

Keywords: AC impedance analysis; Chalcogenide glass; Glassy electrolyte; $\text{Li}_2\text{S}-\text{SiS}_2-\text{Li}_4\text{SiO}_4$; Lithium ion conduction

1. Introduction

In recent years, lithium secondary batteries have been expected for the power sources of the electronic devices, because of their high energy density due to high discharge voltage. In almost all the researches on lithium secondary batteries, organic electrolytes have been used; however, the use of organic electrolytes may cause a lot of technological problems (e.g. leakage, combustibility and electrochemical decomposition) which may not occur when solid electrolytes are used. To overcome these problems, all solid batteries in which solid electrolyte is substituted for liquid electrolyte have attracted much attention [1]. However, no all-solid lithium secondary battery has been commercialized because of poor electrical conductivity of the crystalline solid electrolytes.

On the other hand, it has been reported that glassy solid electrolytes generally have higher ionic conductivity compared to the polycrystalline ceramics at the

same composition [2]. In particular, since some of the chalcogenide glasses have very high ionic conductivity ($\sigma_{\text{RT}} = 10^{-4} - 10^{-3} \text{ S cm}^{-1}$) at room temperature, many researches on these chalcogenide glasses have been carried out. Kennedy et al. [3,4] have investigated the sulfide glass $\text{Li}_2\text{S}-\text{SiS}_2$ and have reported that the doping of lithium halides (LiI, LiCl, LiBr, etc.) into $\text{Li}_2\text{S}-\text{SiS}_2$ glasses improves their ionic conductivity of lithium. However, the doping of lithium halides usually reduces the decomposition voltage in spite of the improvement of the ionic conductivity. Kondo et al. [5–7] have investigated the $\text{Li}_2\text{S}-\text{SiS}_2-\text{Li}_3\text{PO}_4$ glass system, prepared by both the liquid-nitrogen quenching and the twin-roller quenching methods, and have reported that the doping of Li_3PO_4 enhances the ionic conductivity without reducing the decomposition voltage. They also have reported that a lithium secondary battery enables the charge-discharge processes with practical current densities ($> 200 \mu\text{A}/\text{cm}^2$) by using these glasses as the electrolyte. Tatsumisago et al. [8] also have prepared the Li_3PO_4 -doped $\text{Li}_2\text{S}-\text{SiS}_2$ glasses by using a twin-

*Corresponding author.

roller quenching method and have reported that the doping of Li_3PO_4 improves both the stability against crystallization and the ionic conductivity of the Li_2S – SiS_2 glass. Also, Hirai et al. [9] have prepared the Li_xMO_y -doped Li_2S – SiS_2 ($\text{Li}_x\text{MO}_y = \text{Li}_4\text{SiO}_4$, Li_2SO_4) glasses by using a twin-roller quenching method and have reported that the $(1-y)[0.6\text{Li}_2\text{S}$ – $0.4\text{SiS}_2]$ – $y\text{Li}_4\text{SiO}_4$ glass has achieved very high ionic conductivity ($\sigma_{\text{RT}} = 2 \times 10^{-3} \text{ S cm}^{-1}$ at 25°C) at room temperature.

In the present study, we prepare the Li_4SiO_4 -doped Li_2S – SiS_2 glasses with the liquid-nitrogen quenching method and discuss how the doping of Li_4SiO_4 and the different cooling rates influence the ionic conductivity and thermal properties.

2. Experimental

Li_4SiO_4 was prepared by a solid-state reaction of Li_2CO_3 (99.5%) and SiO_2 (99.9%, Soekawa Chemicals) in a molar ratio of 2 : 1. The mixture was calcined at 800°C for 2 h followed by annealing at 1000°C for 2 h in air. The phase was identified by the powder X-ray diffraction. Li_4SiO_4 , Li_2S (99.9%) and SiS_2 (99.9%, Soekawa Chemicals), were mixed in appropriate ratios, and the mixture was put into a carbon crucible and heated at 1000°C for 10 min under N_2 atmosphere. The crucible containing molten glass was dropped into liquid nitrogen to quench it. Since the obtained glasses were so sensitive to moisture, the phase identification of the glasses by X-ray diffraction was carried out by covering the sample with an Al foil.

Ionic conductivity of the glasses was measured by the AC impedance technique. The obtained glassy lumps were cut into pellets. Carbon paste was painted on both sides of the pellet as the electrode. Complex impedance was measured using L.F. impedance analyzer 4192A (HP) in dry N_2 gas in the (20 – 160°C) temperature range. The frequency range was from 5 to 1.3×10^7 Hz.

Glass transition temperature (t_g) and crystallization temperature (t_c) were measured by DTA apparatus (TGD9600, Sinku-riko) at a scanning rate of $20^\circ\text{C}/\text{min}$ in dry N_2 gas.

FT-IR measurement (FTIR-700 spectrometer, JASCO) was performed by the KBr method. The spectrum was obtained in the 400 to 4600 cm^{-1}

region. All the handling was carried out in a glove box under dry N_2 (99.999%) gas.

3. Results and discussion

The homogeneous region of the pseudo-binary glass system $x\text{Li}_2\text{S}$ – $(1-x)\text{SiS}_2$ has been reported to be over the range of $0 \leq x \leq 0.6$ when the glass was quenched by liquid-nitrogen quenching technique [10]. However, we could make a glass only when $x = 0.6$ in the present study. Therefore, Li_4SiO_4 was doped into the $0.6\text{Li}_2\text{S}$ – 0.4SiS_2 glass. The $0.6 \text{ Li}_2\text{S}$ – 0.4SiS_2 glass was greenish yellow and transparent, and the color changed to brown or dark red when Li_4SiO_4 was doped. No X-ray diffraction peak was observed in the glasses with $y \leq 0.075$ in $(1-y)[0.6\text{Li}_2\text{S}$ – $0.4\text{SiS}_2]$ – $y\text{Li}_4\text{SiO}_4$ glass system; however, the glassy samples with $y \geq 0.08$ were not transparent and showed several peaks of Li_2S in the powder X-ray diffraction. Also, the glasses with $y \leq 0.075$ showed glass-transition phenomena in the DTA profiles. From these results, the glass forming region was determined to be $0 \leq y \leq 0.075$. Hirai et al. [9] have reported that the glass-forming region is observed to be $0 \leq y \leq 0.2$ in the same $(1-y)[0.6\text{Li}_2\text{S}$ – $0.4\text{SiS}_2]$ – $y\text{Li}_4\text{SiO}_4$ glass system using a twin-roller quenching technique. The difference in the glass-forming region would be caused by the difference in the cooling rate. Usually, the twin-roller quenching enables a cooling rate faster than that of the liquid-nitrogen quenching.

Fig. 1 shows a typical DTA profile ($y = 0.03$). The glass-transition temperature (t_g) and the crystallization temperature (t_c) were evaluated as shown in this figure. Fig. 2 shows the variations of both t_g and t_c with Li_4SiO_4 composition (y). t_g exhibited a maximum at $y = 0.03$, while t_c exhibited a maximum at $y = 0.06$. Generally, when a glass-network modifier (Li_2S , Ag_2S , etc.) is doped into glass matrix, a restriction in the motion of glass network such as Si – S – Si becomes loose because the modifier cuts the glass network, and t_g shifts to lower temperature side. Actually, when the amount of the glass-network former (SiS_2 , GeS_2 , etc.) increases in glass matrix, t_g rises [11,12]. However, t_g showed a maximum at $y = 0.03$ in the present study, suggesting that the doped Li_4SiO_4 plays a different role from that of a simple glass-

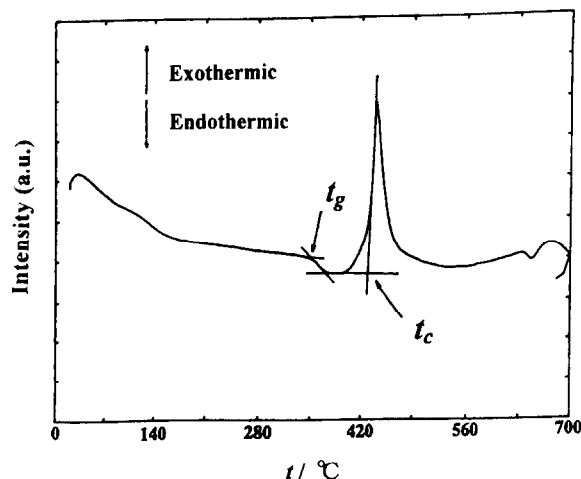


Fig. 1. DTA profile for the $0.97[0.6\text{Li}_2\text{S}-0.4 \text{SiS}_2]-0.03\text{Li}_4\text{SiO}_4$ glass.

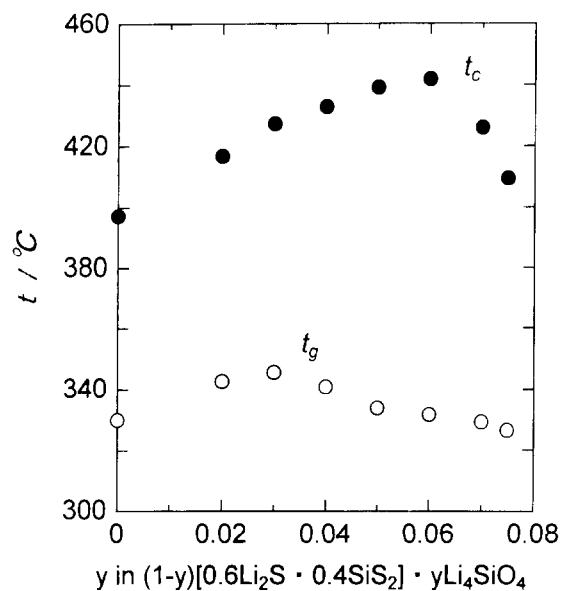


Fig. 2. Variations of glass-transition temperature (open circles) and crystallization temperature (solid circles) with y .

network modifier. Tatumisago et al. [13] have investigated the network structure of $\text{Li}_2\text{S}-\text{SiS}_2-\text{Li}_3\text{PO}_4$ and $\text{Li}_2\text{S}-\text{SiS}_2-\text{Li}_4\text{SiO}_4$ glass system with NMR technique and have found that silicon atoms, coordinated with both sulfur and oxygen, are present in these glass structures when a small amount of Li_4SiO_4 or Li_3PO_4

is doped. They also have reported that various structural units with silicon atoms surrounded by both sulfur and oxygen atoms influence the glass structure and enhance both the ionic conductivity and stability against crystallization of the $\text{Li}_2\text{S}-\text{SiS}_2$ glass. Also, in the present study, such structural units may have been formed and the glass structure may have become more stable by doping Li_4SiO_4 . This means that the doped SiO_4^{4-} ions work as a part of glass former which stabilizes the structure. However, this stabilizer effect of the glass structure would have lasted only up to $y = 0.03$ because t_g exhibited a maximum at $y = 0.03$.

Fig. 3 shows the variation of IR-absorption spectra with y ($y = 0, 0.03, 0.05$ and 0.075). There are three absorption bands in the spectrum of $0.6\text{Li}_2\text{S}-0.4\text{SiS}_2$ glass (Fig. 3, $y = 0$). The frequency peak at 920 cm^{-1} can be identified as the stretching vibration for the Si–S–Si bridging bond (Fig. 3(a)). The peak near 670 cm^{-1} can be assigned as the stretching vibration for the Si–S[−] bond (nonbridging sulfur, Fig. 3(b)). The lower frequency peak at 560 cm^{-1} can be identified as the bond-bending vibration for Si–S–Si bond

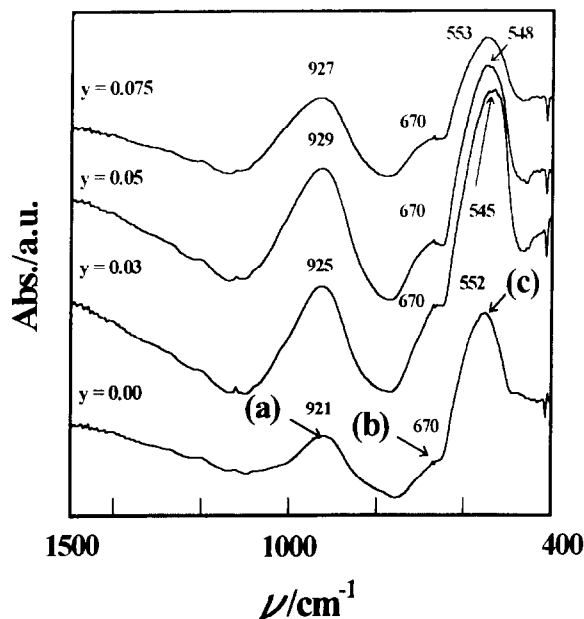


Fig. 3. IR spectra for the $(1-y)[0.6\text{Li}_2\text{S}-0.4\text{SiS}_2]-y\text{Li}_4\text{SiO}_4$ glasses ($0 \leq y \leq 0.075$). (a) – the stretching vibration for the Si–S–Si bridging bond; (b) – the stretching vibration for the Si–S[−] bond; and (c) – the bond bending vibration for Si–S–Si bond.

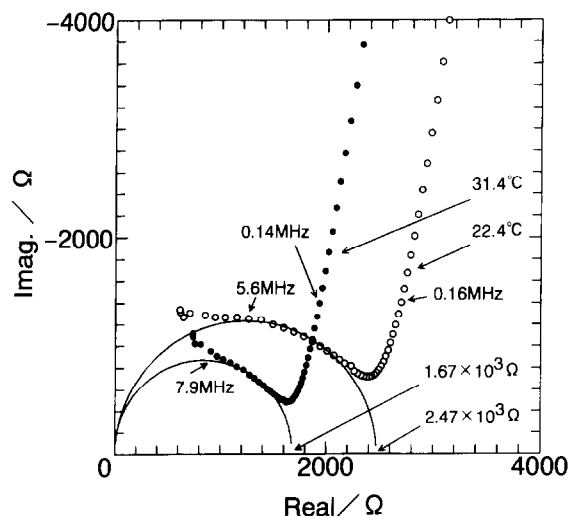


Fig. 4. Complex impedance plots of the 0.97[0.6Li₂S–0.4SiS₂]-0.03Li₄SiO₄ glass.

(Fig. 3(c)) [6,10]. When Li₄SiO₄ was doped into Li₂S–SiS₂ glass, the stretching vibration peak for the Si–S–Si bridging bond (Fig. 3(a)) shifted toward a higher frequency, up to $y = 0.05$ in the present study, indicating that the force constant for the Si–S(O)–Si bridging bond increased due to the formation of the structural unit with silicon atoms surrounded by both sulfur and oxygen atoms. This would be another proof that the doped Li₄SiO₄ worked as a stabilizer of the glass structure. This peak slightly moved to a lower frequency at $y = 0.075$. No clear change in the peak of the stretching vibration for the Si–S⁻ bond (Fig. 3(b)) was observed. On the other hand, the dependence of the bond-bending vibration peak (Fig. 3(c)) on y was rather complicated; however, the reason is still unknown.

Fig. 4 shows the complex impedance plots at the composition of $y = 0.03$. The bulk resistance was obtained from the intersection of the extrapolated semicircle with the real axis at the lower frequency side. Fig. 5 shows the typical reciprocal temperature dependence of ionic conductivity (Arrhenius plots) for typical values of, namely $y = 0, 0.03$ and 0.075 . All the profiles showed an almost linear relation. The variations of the ionic conductivity at room temperature (σ_{RT} at 25°C) and the activation energy (E_a) of ionic conduction with y are shown in Fig. 6. σ_{RT} exhibited a maximum ($1.5 \times 10^{-3} \text{ S cm}^{-1}$) at

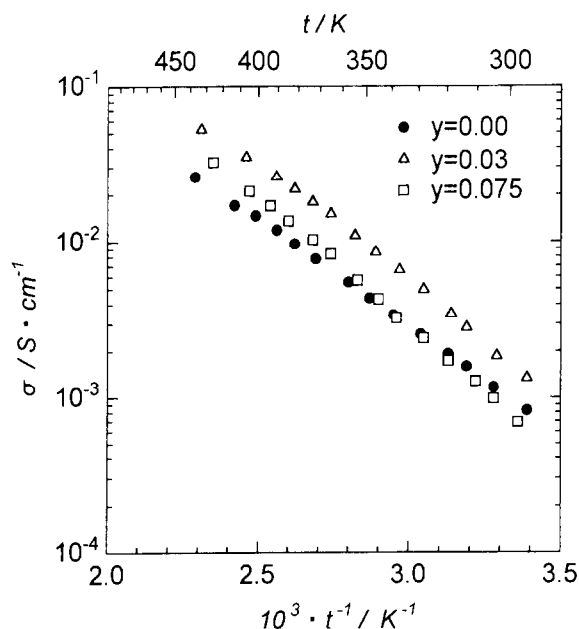


Fig. 5. Typical Arrhenius plots of the ionic conductivity for the $(1-y)[0.6 \text{ Li}_2\text{S}-0.4\text{SiS}_2]-y\text{Li}_4\text{SiO}_4$ glasses.

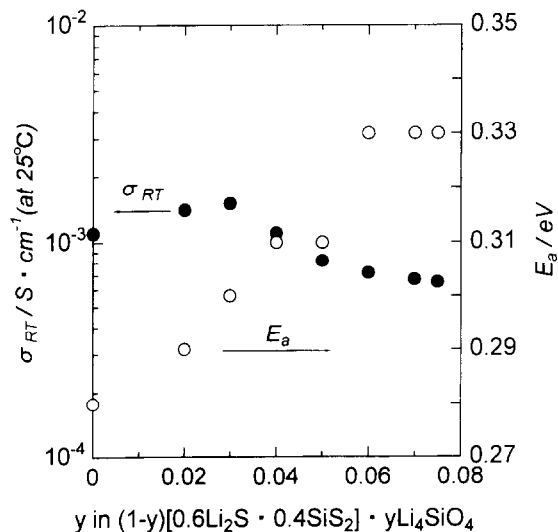


Fig. 6. Variations of the ionic conductivity at room temperature σ_{RT} (25°C; solid circles) and the activation energy E_a of ionic conduction (open circles) with y .

$y = 0.03$. Since this value is comparable to that of Hirai et al. [9], the effect of the difference in the cooling rate on σ_{RT} would be small. Also E_a monotonously increased up to 0.06 with increasing y . In

Table 1
Thermal properties and ionic conductivity at room temperature in the $(1 - y)[0.6\text{Li}_2\text{S}-0.4\text{SiS}_2]-y\text{Li}_4\text{SiO}_4$ glass system

y	$\sigma_{\text{RT}}/\text{S cm}^{-1}$ (25°C)	E_a/eV	$t_g/^\circ\text{C}$	$t_c/^\circ\text{C}$	$t_c - t_g/^\circ\text{C}$
0.00	1.1×10^{-3}	0.28	330	397	67
0.02	1.4×10^{-3}	0.29	343	417	74
0.03	1.5×10^{-3}	0.30	346	427	82
0.04	1.1×10^{-3}	0.31	341	433	92
0.05	8.2×10^{-4}	0.31	334	439	105
0.06	7.2×10^{-4}	0.33	332	442	110
0.07	6.7×10^{-4}	0.33	329	426	97
0.075	6.5×10^{-4}	0.33	326	410	83

general, when the mobile cation is surrounded by the anion network with a strong polarizability, the ionic conductivity increases while the activation energy for ionic conduction decreases [14,15]. Therefore, E_a increases with increasing amounts of introduced Si–O[−] bond because the polarizability of oxygen atom is smaller than that of sulfur atom. However, since the amount of mobile cation (Li⁺) increases due to the doping of Li₄SiO₄, when the amount of doped Li₄SiO₄, when the amount of doped Li₄SiO₄ is small, σ_{RT} may have increased and exhibited a maximum at $y = 0.03$.

Tatsumisago et al. [8] have found that the difference between t_c and t_g ($t_c - t_g$), which represents stability against crystallization, and shows a maximum at $y = 0.05$, where σ_{RT} exhibits the maximum in the $(1 - y)[0.6\text{Li}_2\text{S}-0.4\text{SiS}_2]-y\text{Li}_3\text{PO}_4$ glass system and that the values of σ_{RT} increase with increasing values of $(t_c - t_g)$. Hirai et al. [9] have also reported that the both values of σ_{RT} and $(t_c - t_g)$ show maxima at $y = 0.05$ in the $(1 - y)[0.6\text{Li}_2\text{S}-0.4\text{SiS}_2]-y\text{Li}_4\text{SiO}_4$ glass system. However, in the present study, $(t_c - t_g)$ exhibited a maximum at $y = 0.06$, and no clear correlation between σ_{RT} and $(t_c - t_g)$ was observed. The present results would suggest that the ionic conductivity of the $(1 - y)[0.6\text{Li}_2\text{S}-0.4\text{SiS}_2]-y\text{Li}_4\text{SiO}_4$ glass at room temperature correlates more strongly with t_g (Table 1). Further investigation will be necessary to elucidate this problem.

4. Conclusion

Chalcogenide glasses $(1 - y)[0.6\text{Li}_2\text{S}-0.4\text{SiS}_2]-y\text{Li}_4\text{SiO}_4$ were synthesized by liquid nitrogen quench-

ing method. The glass-forming region was determined to be $0 \leq y \leq 0.75$. t_g and t_c showed maxima at $y = 0.03$ and 0.06 , respectively. Also, when Li₄SiO₄ was doped into Li₂S–SiS₂ glass, a slight peak shift toward a higher frequency was observed in the FT-IR spectrum, resulting from the increase of the force constant due to the formation of the structural unit with silicon atoms surrounded by both sulfur and oxygen. From these results, it seems that the doping of Li₄SiO₄ enhances the thermal stability of the glass structure. E_a monotonously increased with increasing amounts of doping Li₄SiO₄; however, σ_{RT} showed a maximum ($1.5 \times 10^{-3} \text{ S cm}^{-1}$; 25°C) at $y = 0.03$. This is one of the highest ionic conductivity reported so far for a variety of solid electrolytes. It seems that doping Li₄SiO₄ improves the ionic conductivity of Li₂S–SiS₂ glass.

References

- [1] K. Kanehori, K. Matsumoto, K. Miyauchi and T. Kudo, *Solid State Ionics*, 9/10 (1983) 1445.
- [2] A.M. Glass, K. Nassau and D.H. Olson, in: P. Vashishta, J.N. Mundy and G.K. Shenoy (Eds.), *Fast Ion Transport in Solids*, North-Holland, Amsterdam, 1979, p. 707.
- [3] J.H. Kennedy, S. Sahami, S.W. Shea and Z. Zhang, *Solid State Ionics*, 18/19 (1986) 368.
- [4] J.H. Kennedy and Z. Zhang, *J. Electrochem. Soc.*, 135 (1988) 859.
- [5] S. Kondo, K. Takada and Y. Yamamura, *Solid State Ionics*, 53–56 (1992) 1183.
- [6] N. Aotani, K. Iwamoto, K. Takada and S. Kondo, *Solid State Ionics*, 68 (1994) 35.
- [7] K. Iwamoto, N. Aotani, K. Takada and S. Kondo, *Denkikagaku*, 63(1) (1995) 25.
- [8] M. Tatsumisago, K. Hirai, T. Minami, K. Takada and S. Kondo, *J. Ceram. Soc. Japan*, 101(11) (1993) 1315.

- [9] K. Hirai, M. Tatsumisago and T. Minami, *Solid State Ionics*, 78 (1995) 269.
- [10] J.H. Kennedy and Y. Yang, *J. Solid State Chem.*, 69 (1987) 252.
- [11] A. Pradel and M. Ribes, *Solid State Ionics*, 18/19 (1986) 351.
- [12] B. Carette, E. Robinel and M. Ribes, *Glass Technology*, 24 (1983) 157.
- [13] M. Tatsumisago, K. Hirai, T. Hirata, M. Takahashi and T. Minami, 10th International Conference on Solid State Ionics, Singapore, 1995, p. 256, extended abstracts.
- [14] D. Ravaine, *J. Non-Crystalline Solids*, 38/39 (1980) 353.
- [15] M. Ribes, B. Barrau and J.H. Souquet, *J. Non-Crystalline Solids*, 38/39 (1980) 271.